A Novel Quantitative Approach to Positron Emission Tomography for the Diagnosis of Alzheimer's Disease

By

Audrey Katako

A Thesis Submitted to the Faculty of Graduate Studies of

The University of Manitoba

In partial fulfilment of the requirements of the degree of

MASTER OF SCIENCE

Department of Human Anatomy and Cell Science

University of Manitoba

Winnipeg

Abstract

The incidence of Alzheimer's disease (AD) amongst the elderly in Canada (age >65) is expected to grow with increasing life expectancy. Current diagnostic methods are qualitative and yield equivocal results whose unreliability is exacerbated by variations in physician experience and technique. Therefore, there is a need for a quantitative method for interpreting Positron Emission Tomography (PET) brain scans. The method should be sensitive, specific, and capable of distinguishing between affected and unaffected individuals even in early disease stages. Here, scaled subprofile modeling/principal component analysis (SSM/PCA) and machine voting were used with 763 subjects from the Alzheimer's disease Neuroimaging Initiative database and 99 subjects referred to the Health Sciences Centre – Winnipeg PET center between 2010 and 2012 to generate a machine voting score for Alzheimer's disease (MVAD), which can distinguish between progressors and non-progressors from mild cognitive impairment to AD.

Acknowledgements

The completion of this thesis and the attainment of the degree of Master of Science in Human Anatomy and Cell Science would not have been possible without the incredible opportunity afforded to me by Dr. Ji Hyun Ko. As a mentor and advisor, he not only made my studies financially possible, but also served as an incredible example of a successful, hardworking, and innovative research scientist; truly an individual with a mind and work ethic to both admire and emulate.

The support of my lab colleagues, Dr. Maram Aljuaid and Dr. Dali Zhang, was instrumental in the completion of the project which has led to the composition of this thesis.

With the support and expertise of my advisory committee members, Dr. Hugo Bergen, Dr. Maria Vrontakis-Lautatzsis, and Dr. Andrew Goertzen, my journey as a graduate student was truly enriched.

Dr. Paul Shelton and Ms. Erica Sheffield of Crescentwood Memory Clinic in Winnipeg, Manitoba played an essential role in this project through their clinical expertise and willingness to support this project with their efforts.

I would also like to extend my gratitude to the Dr. Paul H.T. Thorlakson Foundation, as well as the University of Manitoba and the Alzheimer Society of

Manitoba, without whose financial support this project would have been impossible.

Dedication

To my magnificent parents, whose unwavering support and patience have fueled my passion for science and for furthering my education. I owe you everything and more.

For John, who is truly my best friend and partner. You abound with endless encouragement, faith, love, and support.

My dear sister Rollina: there aren't many sisters like you. I'm so grateful for all you've done and I can never thank you enough.

For my grandfather, the first to pick up a book and plant the seeds of love and respect for education: you opened the door for me long before I was even a glint in my father's eye.

Table of Contents

List of Tables

List of Figures

Table of Abbreviations

Abbreviation	Definition
Aβ	Amyloid beta
AD	Alzheimer's disease
ADRP	Alzheimer's disease Related Pattern
DLB	Dementia with Lewy Bodies
EOAD	Early-Onset Alzheimer's disease
FTD	Frontotemporal dementia
FDG-PET	Fluorodeoxyglucose positron emission tomography
MCI	Mild Cognitive Impairment
MMSE	Mini-Mental State Examination
MRI	Magnetic Resonance Imaging
MVAD	Machine Voting Alzheimer's Disease Score
PDD	Parkinson's disease Dementia
SSM/PCA	Scaled Subprofile Modeling/Principal Component Analysis

1. Introduction

Currently, and based on clinical and methodological consensus, 18-Fluorodeoxyglucose (FDG) Positron Emission Tomography (PET) is the most widely used brain imaging modality that complements diagnosis of Alzheimer's disease (AD) [2]. AD patients exhibit declines in FDG uptake within the parietotemporal, frontal and posterior cingulate cortices when compared to normal age-matched controls. There exists, however, significant individual variation in patient PET signals expressed which limits the use of a definitive threshold for FDG-PET in AD diagnosis. Therefore, the nature of the clinical reading of FDG-PET images is usually based on subjective impressions of the relative hypo-metabolism in key anatomical brain regions. Consequently, no quantifiable biomarker-related numeric value is produced and as a result it is often concluded that reports are equivocal. In addition, the sensitivity of subjective readings at an early disease stage remains challenging, while relatively high accuracy can be achieved for more advanced stages [2].

Three-Dimensional Stereotaxic Surface Projection (3D-SSP), is a PET imaging analysis platform which makes use of region-of-interest (ROI) Z-scores to create a glucose metabolism/disease specific statistical brain map which is then used to determine the likely disease state of the patient [3]. While this technique is both advanced and innovative, it does not, however produce a quantitative outcome

for the entire brain network that is relevant to AD. Thus, the imaging report using 3D-SSP is bound to be descriptive limited to different ROIs. It is also incapable of taking into account network interactions that have been demonstrated to be important, given that there is a large body of literature discussing the role of resting state brain network abnormalities associated with AD [4-6]. Brain network connectivity has been found to be impaired in AD patients, with these subjects exhibiting lower levels of functional connectivity due to increased amyloid deposition, a link between protein and pathology which is being explored in ongoing research [7].

Alternative diagnostic approaches include the use of a PET radiotracer that binds to AD pathology-specific proteins such as beta-amyloid (Aβ) and phosphorylated tau. The invention of Pittsburgh Compound-B (PiB) [8] and other second-generation Aβ radioligands has been heavily researched within the field of molecular imaging over the past decade. Meta-analysis on longitudinal PiB studies estimates 94.7% sensitivity but 57.2% specificity [9] which implies high false positive rates of Aβ-PET. This confounding factor is inevitable since it has been estimated that approximately 20-30% of cognitively normal subjects exhibit abnormally high levels of high Aβ protein [10]. For this reason, the purpose of the recent on-going IDEAS study (Imaging Dementia-Evidence For Amyloid Scanning; http://www.ideas-study.org), in which the benefit of Aβ-PET will be

evaluated for Medicare coverage, had to be limited to assessing Aβ status rather than AD status. A number of groups are currently investigating tau-imaging agents with promising results in some instances, but more rigorous testing needs to be done in upcoming years for these radioligands to be proven to be of any notable clinical significance that can be translated into clinical utility in a healthcare setting [11].

The arena of neuroimaging as it pertains to its use in the diagnosis of AD is growing further still with the possible introduction of PET radiotracers that study other pathological signs of AD such as neuroinflammation, which is elevated in AD patients and can be quantified with the use of radiotracers such as, [^{11}C](*R*)PK11195 [12], [11C]-PBR28 [13], [11C]-DPA-713[14] and [18F]-FEPPA [15], all of which bind to the brain's translocator protein (TSPO) mitochondrial protein receptors.

In a combined effort involving multiple research centers in North America, the AD Neuroimaging Initiative (ADNI) has collected the largest available multi-modal longitudinal brain imaging database for patients with AD, Mild Cognitive Impairment (MCI) and normal control subjects (http://www.adni-info.org/Home.aspx). Utilizing the ADNI database, Shaffer et al. [16] assessed the predictive utility of each proposed AD biomarker for structural magnetic resonance imaging (MRI), spinal tau concentration and FDG-PET. The authors concluded

that FDG-PET provided the most prognostic information. In this seminal report, independent component analysis (ICA) was employed and it produced characteristic brain metabolic patterns that distinguished between MCI patients at baseline who progressed to AD and those who did not.

Forward computation of scaled subprofile modeling (SSM) [17] - a form of principal component analysis (PCA), in FDG-PET has proven to be useful for differential diagnosis and prognosis in other neurodegenerative disorders [18-20]. Unlike ICA, PCA's scale is not arbitrary, thus topographic profile ratings, i.e., topographical similarity between the disease-related metabolic pattern and a single FDG-PET image, which is defined as subject scores of the given pattern, can be accurately estimated in individuals whose FDG-PET images were not used in the original pattern derivation [1]. The use of machine voting in the form of random permutations and voting strategies (see Method for details) adds further stability and abolishes potential biases which can be originated from the selection of training sets. Here, we utilize both machine voting and SSM/PCA as a lofty tool with heightened utility in the accurate classification of patients into disease groups, when the two are employed in tandem.

In the current study, we revisited the use of a well-established multivariate analysis technique (i.e., SSM/PCA) for the quantitative readings of FDG-PET.

Since the disease-related pattern identified by SSM/PCA is dependent on the definition of the derivation set, we proposed a novel machine-voting-based approach adding onto the current SSM/PCA, and evaluated its performance as an imaging-based biomarker for AD using both cohorts from ADNI database and a local PET clinic to demonstrate its translational feasibility.

2. Background

AD is the most prevalent cause of dementia that affected 47 million people around the globe as of 2015[21]. This number is expected to balloon to 130 million affected worldwide by 2050. The current economic toll of the disease currently exceeds USD 818 million [21]. Early detection of AD may benefit both patients and caregivers by providing a better chance of benefiting from treatment, relief from anxiety about unknown problems, ample time to plan for the future and timely access to psychosocial education [22].

First identified in 1906 by German psychiatrist Aloïs Alzheimer, AD is an incurable, debilitating neurodegenerative disease that is responsible for over 70% of all dementia cases in the elderly across the globe [23]. It is believed that the neurological changes which take place in the brain at a molecular level begin at a young age, sometimes decades before the first cognitive changes are detectable [24]. The pathological process of dementia due to AD is such that it has two primary causative agent molecules: phosphorylated tau protein and insoluble

aggregates of the protein amyloid beta (Aβ) [25]. Symptoms of AD include an array of cognitive deficiencies such as memory loss, confusion and depression, as well as wandering [26]. The disease is diagnosed through the administration of neuropsychological testing and clinical interviews to determine cognitive function. Brain FDG-PET scanning is utilized to a lesser extent in clinical practice, but has been established to be the gold-standard in AD neuroimaging [27]. There is currently no cure for AD and the foremost palliative treatment for the disease is the administration of drugs in the class of the acetylcholinesterase inhibitor [28]. In an effort to further the understanding of the connection between mild cognitive impairment (MCI) and AD, the Alzheimer's Disease Neuroimaging Initiative (ADNI) was set up in 2004 with the mission of creating a database of normal, MCI and AD subjects to track AD progression across the elderly population in North America [29].

2.1 Clinical Expression

AD occurs in four stages that correlate with the level of cognitive impairment observed in the affected individual. The first, termed early cognitive impairment, occurs approximately ten to fifteen years before the appearance of physical symptoms. The subsequent stage is called mild cognitive impairment and can often overlap with late mild cognitive impairment, a condition usually leading directly to clinical AD or another form of dementia. The condition of an individual in either

of these two stages is expected to progress to the stage of clinically discernible AD, the final stage of the illness, with an estimated 15% of all MCI sufferers converting to AD annually [30].

Some of the physical symptoms that are observed in an individual with AD include the inability to perform familiar tasks, poor recall of recently learned material, personality changes such as reclusiveness and apathy, aimless wandering, and the inability to articulate one's thought in the form of intelligible speech. Symptoms are progressive and worsen as the disease takes its course. They are commonly first observed by those close to the patient and who notice unusual behaviors, prompting the seeking of medical attention.

From a histological standpoint, AD is characterized by the presence of two types of protein deposits observed in the brain. The first is the accumulation of insoluble plaques composed of the protein Aβ that aggregate in the cerebral cortex as a result of the failure of the mechanism responsible for removing the protein from the brain [31]. The second is the formation of fibrous neurofibrillary tangles which form inside neuronal cells as the protein named tau becomes dysfunctional and is amassed in clumps within the neuron [32]. The brain also begins to exhibit marked atrophy with brain mass being severely reduced in later stages of the disease [33]. The formation of both of these pathological hallmarks remains poorly understood. However, their presence alone points to failures in mechanisms meant

to remove unwanted material from the brain. Aβ protein aggregations bind to chemoreceptors on glia and astrocytes, initiating an immune response which culminates in the release of molecules involved in neuroinflammation. There is an established interplay between inflammation and protein accumulation [34]. **Figure 1** depicts this process.

Figure 1

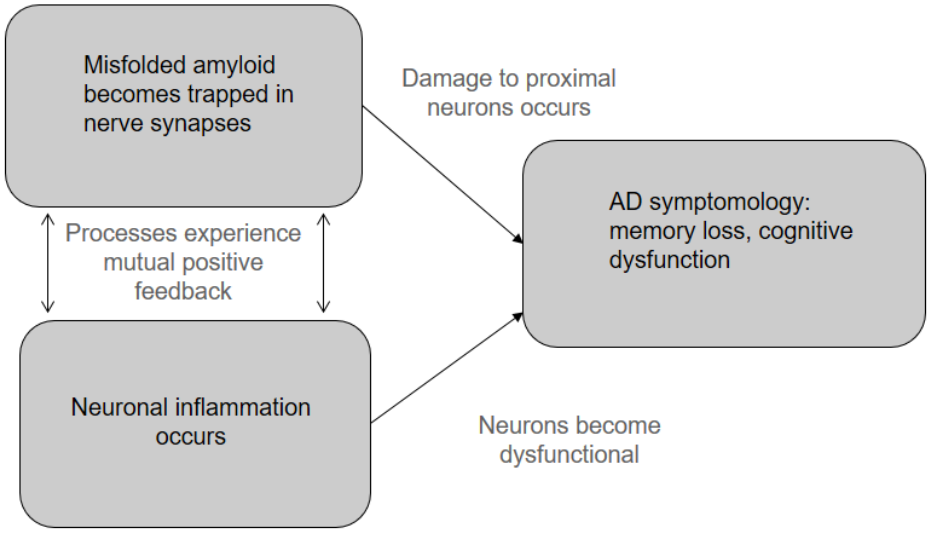

Figure 1: Depiction of the process of amyloid-beta aggregation within neuron synapses coupled with the inflammation of neurons, the combination of which results in the clinical symptoms observed in AD. Adapted from [35].

2.2 Epidemiology

The current estimated incidence of AD is believed to 24 million total cases worldwide, with the vast majority of diagnosed cases occurring in North America and Western Europe with respective prevalence rates in the over-60 population of 6.4% and 5.4%. By 2040, it is expected that some 48 million total individual cases will have been diagnosed due to an increased level of aging in the developed world [36].

There are a number of established risk factors for AD which include age older than 65 years, a medical history which includes diabetes and/or hypertension, and being genetically homozygous for the APOE E4 allele. Conversely, neuroprotective factors which decrease the overall risk of developing AD include maintaining a low dietary intake of saturated fats, as well as engaging in mentally stimulating activities such as gardening [37].

While late-onset AD occurs in individuals aged >65, a variant of the disease termed early-onset AD (EOAD) afflicts individuals as young as 40 years old. It is the most common form of dementia observed in individuals below 65 and has an estimated non-familial prevalence of 4-6% in total AD cases [38]. A number of genes have been implicated in familial EOAD such as a mutation in presenilin 1

(*PSEN1*), which is the most common cause of familial EOAD and is responsible for some 182 individual gene mutations, as well as the genes *PSEN2* and *APP* [39].

2.3 Current State of Diagnosis

A number of criteria need to be met before a diagnosis of AD can be conferred. Since 1984, and with a revision in 2011, the National Institute of Neurological and Communicative Disorders and Strokes and the Alzheimer's disease and Related Diseases Association (NINCS-ADRDA) criteria have been in use. For a patient to receive a diagnosis of probable AD, the following criteria must be met: gradual onset of symptoms over many months or years, and observed worsening of amnestic (inability to recall newly learned information) or nonamnestic (deficits in language, visuospatial reasoning, and executive function) symptoms [40] .

Clinical diagnosis usually involves the use of neuropsychological examinations such as the Mini-Mental State Examination (MMSE)[41], Montreal Cognitive Assessment (MoCA)[42] or Clinical Dementia Rating (CDR) [43] in conjunction with a clinical interview. Diagnosis is sometimes achieved through the incorporation into the clinical workup of PET scanning which reveals decreased glucose metabolism in the frontal, parietal, temporal, and posterior cingulate cortices of the brain. MRI imaging may also be used [44].

The current consensus is that patients with mild cognitive impairment (MCI) are at higher risk of developing AD or other forms of dementia in comparison to age-matched normal controls. Therefore, routine tests of mental/neuropsychological performance and interviews by physicians may be used for early detection of AD [45]. However, only 20-40% of amnestic MCI patients ultimately convert to AD [46]. The use of [^{18}F]fluourodeoxyglucose (FDG) PET, a brain imaging technique that estimates regional glucose metabolism, has been widely accepted as a method that complements traditional clinical diagnosis of AD [2], but the subjective impressions of FDG-PET readings as they are currently interpreted by physicians are often found to be equivocal. Therefore, more objective quantification of risk estimation using FDG-PET is a necessity.

The present method of examining PET scans used by nuclear medicine physicians has not been standardized across Canada, let alone the rest of the globe. Reading techniques vary greatly from one physician to the next, and subsequently even within the same clinical department. This is due to interindividual differences such as the type of training obtained during residency, personal preferences and methodologies, as well as varying levels of training, i.e. being a recently board-certified physician as opposed to a physician with decades of experience. The numerous discrepancies observed introduce a challenge when it comes to differential diagnosis of dementia types and/or its early diagnosis.

FDG-PET is the most widely used brain imaging modality that complements diagnosis of AD [2]. AD patients exhibit declines in FDG uptake in the parietotemporal, frontal and posterior cingulate cortices when compared to normal age-matched controls. Current specificity in a clinical setting rests at approximately 75%, while sensitivity is estimated to be 59%. These findings were made in a 2012 study by Shipley et al. in which PET scans obtained from 46 patients with dementia were examined by two fellowship-trained neurologists at the Neurobehavior Clinic of the University of Colorado Hospital [47].

In the past, disease-specific perfusion/metabolic patterns have been generated by amalgamating well-defined (advanced) patient and age-matched normal controls groups [17]. The rationale is that if there exists a unique representative spatial brain metabolic pattern that characterizes the given disease (i.e., differentiating patients from normal controls), SSM/PCA should be able to characterize it as one of the eigenvectors. Therefore, for the purpose of differential diagnosis across a similar spectrum of diseases (e.g., AD and other types of dementia), it may work best if the disease-specific patterns are defined as a contrast to age-matched normal controls [6].

Another potential challenge lies in distinguishing one form of dementia, which may present with very similar PET readings and symptoms, from another.

Based on the similarities between certain dementia types which were observed during PET scan analysis conducted in this study, there is a great need for improvement in differential diagnostic methods.

Current PET reading methods have been neither standardized nor automated and the interpretation of the clinical significance of the cerebral metabolic rate of glucose is at the discretion of the clinical practitioner. The characteristic topography of the AD brain has been determined to involve decreases in relative metabolic rates within the middle cingulate, superior medial frontal and bilateral parietal cortices [48].

2.4 Treatment of AD

Individuals diagnosed with AD have an average life expectancy of 7-10 years[49]. There is currently no cure for AD and treatment consists of the administration of a cholinesterase inhibitor such as donepezil, memantine or galantamine, as well as other medications that treat comorbid conditions such as depression and anxiety as they manifest. This class of drugs has been found to be successful in decreasing the progressive cognitive decline which characterizes AD in 40-58% of responder cases [50].

The mechanism of action of acetylcholinesterase inhibitors involves a wide range of pharmacologic processes such as the prevention of acetylcholine depletion

within the synaptic cleft, which translates to an overall increase in cerebral acetylcholine levels, as well as encouraging cholinergic neurotransmission [51]. A number of other potential treatments are currently in the research and development pipeline to widen the pool of available drugs. For instance, P7C3, a serotonin antagonist and derivative molecule of an antihistamine called dimebon, has been found to elicit neuroprotection through its binding to the brain's 5-HT6 (serotonin) receptor[52]. In a similar fashion, 6-methyluracil is currently being investigated as a potential treatment for AD due to its inhibitory properties which allow it to successfully prevent Aβ from binding to both its peripheral and catalytic active sites on the acetylcholinesterase molecule, thus impeding its ability to metabolize acetylcholine within neurons[53]. Other potential treatments include the administration of α-melanocyte stimulating hormone[54] and metal-protein attenuating compounds (MPACs) such as PBT2[55].

2.5 Alzheimer's disease Neuroimaging Initiative (ADNI)

The Alzheimer's disease Neuroimaging Initiative (ADNI) is a North American project which seeks to compile a detailed, longitudinal database comprised of comprehensive clinical, genetic and neuroimaging data collected from thousands of AD, MCI and normal subjects across the region with the purpose of tracking AD conversion and progression. It provides a wealth of

information which has formed the basis for a large number of studies that have yielded fruitful results since the project's inception in 2003. A number of valuable discoveries have been made as a result of the depth of the data available within the ADNI. It has provided a platform from which to conduct multicenter studies involving large pools of patients, the development of novel ways of diagnosing early AD through biomarkers such as CSF-tau and amyloid beta levels, as well as encouraged the selective recruitment of clinical trial subjects exhibiting traits that indicate an increased likelihood of AD conversion [56].

Using ADNI or similar large databases, a number of studies have attempted to utilize multivariate analysis to not only achieve increased accuracy of AD diagnosis, but increased accuracy in MCI-to-AD conversion as well. Other multimodal approaches such as those described in [57], [58] and [59], have several barriers to implementation that we expect our method to be able to successfully circumvent, such as the use of CSF-tau and other biomarkers which may be too costly to collect and do not always offer adequate amounts of diagnostic data (e.g. high CSF-tau may be observed in one patient with AD and another with another form of dementia) in a clinical setting as well as the methodological challenge of preventing overfitting of the data.

3. Hypothesis

We investigated the predictive power of the proposed SSM/PCA-machine voting approach in quantitatively identifying those patients who prospectively developed dementia in a clinical setting. It has been previously determined that subjects who are cognitively normal differ in cerebral rate of glucose metabolism (CMRglu) pattern expression as visualized through PET scanning, as do those with MCI, etc. That is to say that dementia, or lack thereof, produces a unique topographical pattern when PET scanning is applied [60]. It has also been established that changes which occur within the brain and which are detectable through the utilization of PET scanning, do not occur at a stand-alone, regional level, and that despite the fact that individual brain regions which are commonly affected in AD have been identified; the changes which occur take place on a global scale within the brain [61]. Consequently, we hypothesized that this divergence in glucose metabolism dependent on disease group classification would not only be evident in AD, MCI and normal controls, but would also be both evident and unique in both prodromal AD and stable MCI subjects involved in this study.

4. Aims

Our aims in this study revolved around two main objectives:

1. To develop a quantitative, voxel-based analytical PET reading method which is able to provide good sensitivity and specificity.
2. To demonstrate the feasibility of applying the proposed diagnostic method in a clinical setting.

We sought to achieve these goals by utilizing two sets of patients with established clinical diagnoses. One group (ADNI) was to be used to generate a disease-related pattern (ADRP) with good discriminative power (sensitivity>70% and specificity >40% specificity) as specified by lower ends of these thresholds [62]. This group was also to be used to test the ability of the pattern to predict MCI to AD conversion due to the availability of a suitably large sample size. The other, regionally-sourced patient group (HSC), was to be utilized as a testing set to establish the translational utility of the derived ADRP as a clinical tool with the potential to be implemented within a regional PET scanning and analysis center.

5. Research Methods

Data used in the preparation of this article were obtained from the Alzheimer's Disease Neuroimaging Initiative (ADNI) database (adni.loni.usc.edu). The ADNI was launched in 2003 as a public-private partnership, led by Principal Investigator Michael W. Weiner, MD. The primary goal of ADNI has been to test whether serial MRI, PET, other biological markers, and clinical and

neuropsychological assessment can be combined to measure the progression of MCI and early AD.

Subjects

A total of 783 subjects from the ADNI database who had available PET and MRI scans were included in this study. ADNI subjects came from one of three groups: AD, normal controls (NC), and MCI. MCI patients were further divided into stable MCI (who did not develop AD during the 3 years of follow-up period) and prodromal AD (who developed AD within 3 years). ADNI subjects had a mean age of 74.0±7.3) and Mini-Mental State Examination (MMSE) score of 27.2±1.7. Demographic details regarding the ADNI cohort are given in **Table 1**. HSC cohort subject demographics are outlined in **Table 2**.

TABLE 1

Characteristic	NL	AD	Stable MCI	Prodromal AD
Number	111	94	186	55
Age	74.5(6.6),56-94	*75.5(8.3),56-90	75.1(6.4),60-87	71.3 (7.7), 55-90
MMSE	29.0(1.2),24-30	*24.2(1.8),20-26	26.9 (1.9), 24-30	28.3(1.6), 24-30
Sex (M: F)	91:107	59:35	99:87	49:43
Follow-Up Duration (months)	40.5(26.8),36.0-121.0	10.4(7.1),0.0-27.0	53.8(36.0),18.2-112.0	53.6(20.2),36.0-107.0

Table 1: Demographic data for patients acquired from the ADNI (Alzheimer's Disease Neuroimaging Initiative) database.

* $p<0.05$, student t-test between NL vs. AD. No variable was significantly different between stable MCI vs. prodromal AD.

TABLE 2

Characteristic	MCI-HSC	AD-HSC	DLB/PDD-HSC	FTD-HSC	VaD-HSC
Number	18	33	18	4	5
Age	70.4 (5.5),62-78	69.1(8.1),48.0-86.0	68.1(8.3),56.0-81.0	64.5(2.12),63-66	76.4(11.9),59-91
MMSE	27.3 (1.8),22-29	23.7(6.2),16-29	24.2(4.7),14-30	28.5(0.7),28-29	23.75(2.6),20-26
Sex (M: F)	7:11	17:16	9:9	3:1	3:2
Follow-Up Duration (months)	59.9(6.0),15.8-90.9	29.8(23.0),0.0-123.6	29.4(23.0)0.0-123.6	63.1(14.7),32.4-108.0	29.0(22.0)22.0-123.6

Table 2: Demographic data for patients referred to the PET Centre at the Health Sciences Centre in Winnipeg, Manitoba. * $p<0.05$, ANOVA including all disease groups. Only MVAD score ($F(4, 73) = 9.078$, $p<0.001$), follow-up period ($F(4,73)=4.915$, $p<0.001$) and MMSE ($F(4,73)=2.100$, $p<0.089$) revealed significant between-group differences. Values are mean, with SD in parentheses and followed by range.

Schematics describing the process of patients sorting and follow-up for the ADNI and HSC cohorts can be found in **Figures 2 and 3**, respectively. Data from a total of 61 patients who had been scanned at the Health Sciences Centre (HSC) in Winnipeg, Manitoba, Canada between 2010 and 2012 were used in this study. HSC subjects were comprised of those who received a final diagnosis of MCI, AD, frontotemporal dementia (FTD), dementia with Lewy Bodies (DLB) or vascular dementia (VaD) after having received a PET scan. HSC subjects had a mean age of

69.5±7.0 with a Mini-Mental State Examination (MMSE) score of 22.1±7.2. The exclusion criteria for both patient sets were lack of a baseline PET scan and lack of follow-up data.

Figure 2

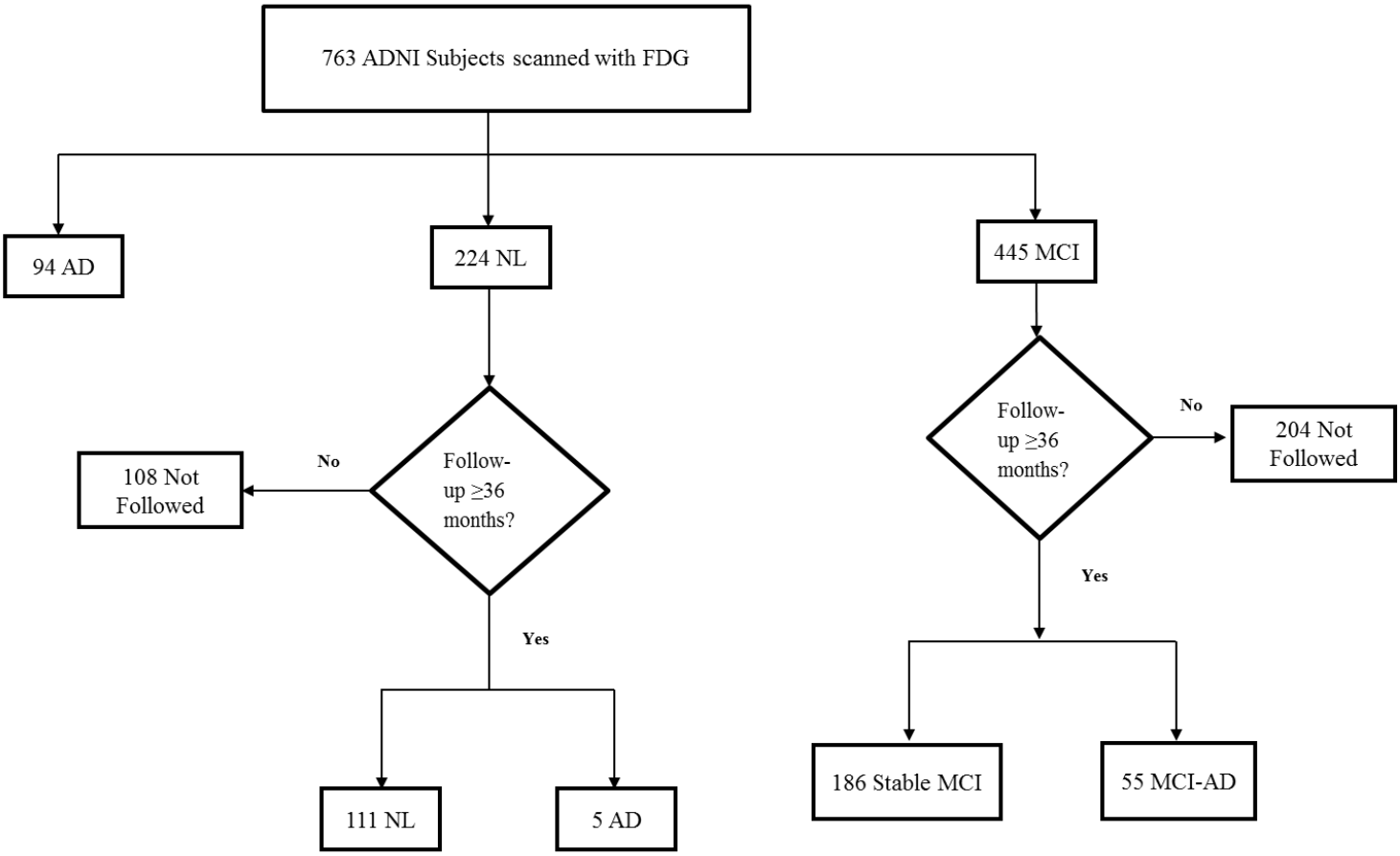

Figure 2: From the ADNI database, we identified three groups of individuals, i.e., patients with AD (AD; n=94), normal controls (NL; n=224), and subjects with mild cognitive impairment (MCI; n=445). Of the 445 MCI subjects selected for this study, 204 were not followed for a period of ≥36 months, and of the remaining 241, 186 remained stable MCI, with 55 subjects converting to AD (prodromal AD) within the 36-month follow-up period. Similarly, 224 NL subjects were studied, and of those 108 were not followed for ≥36 months. Of the remaining 116, 111 remained NL at the end of the follow-up period. Follow-up duration was neglected for AD subjects as dementia was already present at the time of screening.

Figure 3

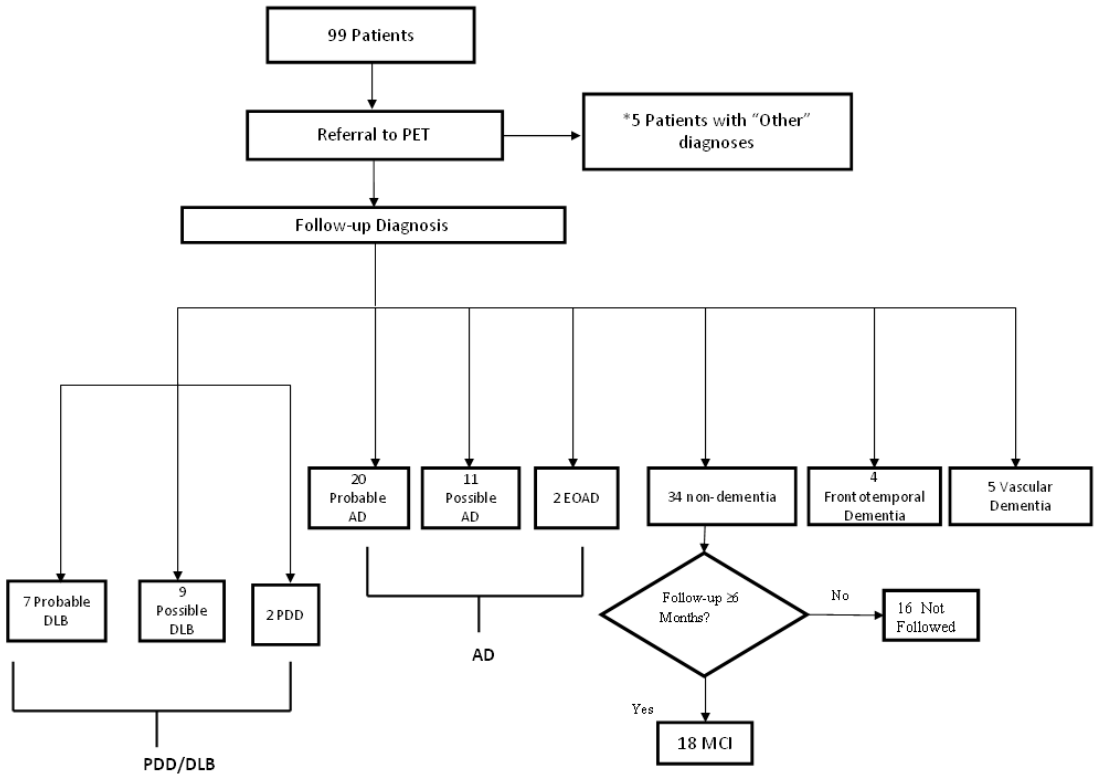

Figure 3: Schematic depicting the diagnostic progression of the HSC cohort both after PET scanning as well as three years after the initial diagnosis of MCI. 33 AD subjects (of these, 20 had probable AD, 11 had possible AD, 2 had early-onset AD) were diagnosed after PET scan, as were 2 Parkinson's disease Dementia (PDD), 16 Dementia with Lewy bodies (DLB, 7 probable and 9 possible), 5 VaD, 4 FTD and 18 MCI subjects. Of the 34 patients with undetermined dementia followed for >6 months, only 18 were diagnosed with MCI. Subjects diagnosed with dementia were not followed as dementia diagnosis had already been confirmed following PET scan. *EOAD = Early-onset AD (AD in patients younger than age 65). Other diagnoses included hydrocephalus, corticobasal syndrome, aphasia, vascular dementia, and closed head injury.

Image Acquisition

ADNI PET images were retrieved from the ADNI Laboratory of Neuroimaging (LONI) database in a format under which images had already been preprocessed through coregistration, averaging, and standardization.

PET Image Preprocessing

All ADNI and HSC FDG-PET image preprocessing was carried out using the standard procedure implemented in the statistical parametric mapping 12 (SPM) software (www.fil.ion.ucl.ac.uk/spm/). Images were normalized by warping to the MNI (Montreal Neurological Institute) standard space using a template available in SPM and then subsequently smoothed using an 8mm Gaussian filter.

FDG-PET images for the HSC cohort, who were scanned between 2010 and 2012, were obtained from the PET Centre at the Health Sciences Centre, Winnipeg, Canada. Subjects were patients of the Crescentwood Memory Clinic in Winnipeg, Manitoba, who were referred to the PET Centre for scanning and subsequently diagnosed and followed by PS. Patients who had not been followed were excluded. All clinical and FDG-PET data retrieval was completed according to the protocol described in the Personal Health Information Act (PHIA), information regarding which can be found at http://www.gov.mb.ca/health/phia/. Ethics approval for this study was granted by the Biomedical Research Ethics

Committee at the University of Manitoba. Informed consent was obtained for all subjects who were enrolled in the study, either from the patient or from an individual designated as having power of attorney over the patient and able to make decisions regarding the patient's health.

To evaluate the effects of enhanced anatomical spatial normalization using structural MRI, ADNI PET images were coregistered to corresponding T1 MRI images that had been preprocessed using an ADNI-regulated protocol (http://adni.loni.usc.edu/methods/mri-analysis/mri-acquisition/), then spatially normalized to the ICBM-MRI template utilizing grey matter, white matter and CSF density maps. Normalized images were smoothed with an 8mm Gaussian kernel. .

Construction of 1,000 ADRPs using SSM/PCA

Following image pre-processing, SSM/PCA was performed as described elsewhere [17] using a customized MATLAB script. Of 111 NL and 94 AD subjects from the ADNI database, 20 subjects from each group were randomly selected and used as a training set to generate an ADRP. If the two randomly selected groups were significantly different in age and/or sex, a random draw was repeated to ensure that the identified FDG-PET pattern reflected the disease. The subject scores were evaluated for the first 5 PCs, then the PC with the best group discrimination (minimum p-value by student t-test) was selected as an ADRP [17]. This process was repeated 1,000 times, thus producing 1,000 different ADRPs

(**Figure 4**). For each ADRP, a receiver-operating curve (ROC) was examined to determine the optimal ADRP score threshold to produce the highest sensitivity × specificity in group discrimination. It should be noted that the performance of ADRPs differed even when the demographic variables were controlled not to be significantly different (**Figure 5**).

Figure 4

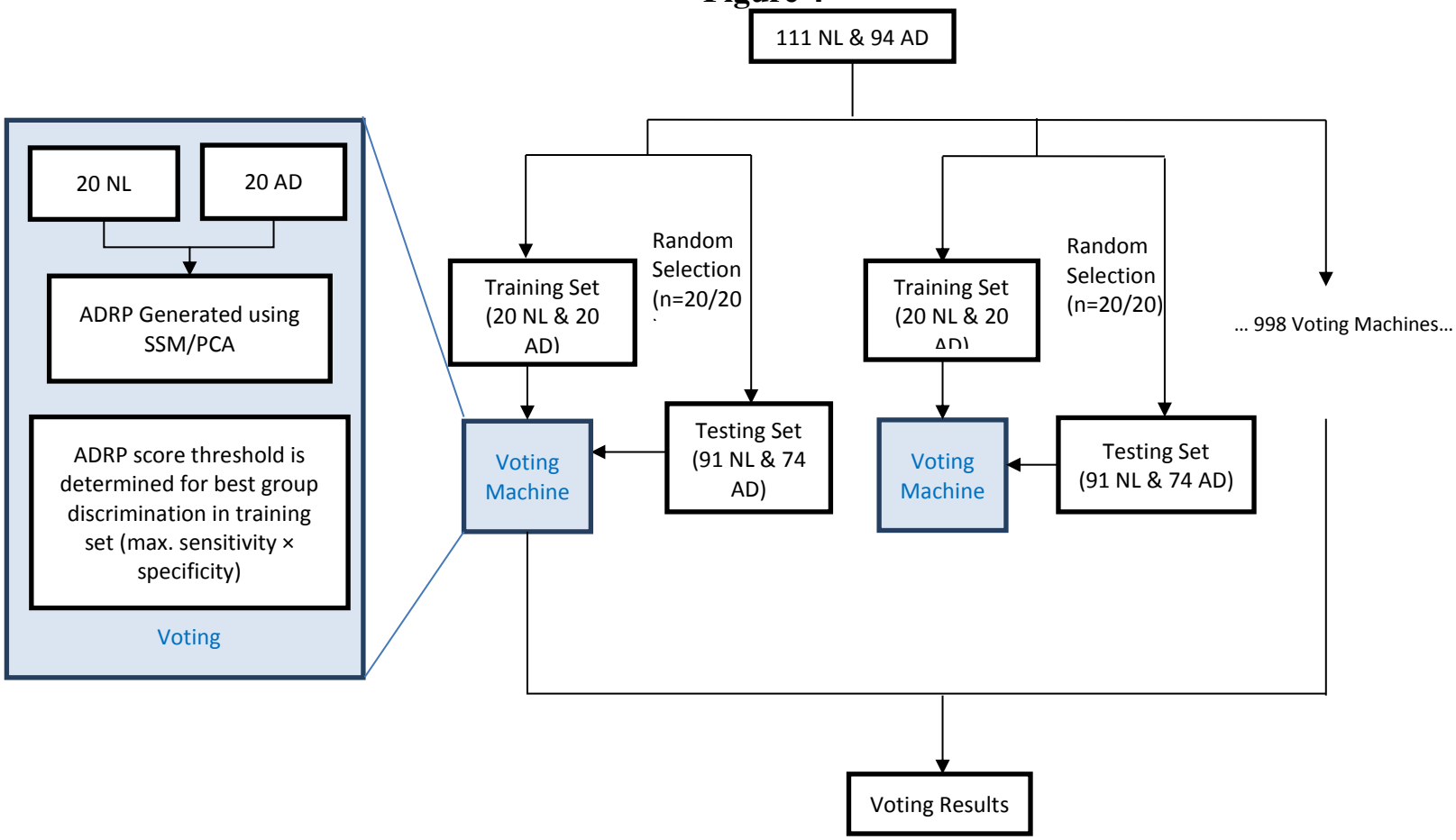

Figure 4: Schematic depicting the machine voting process. Using 1,000 permutations, 20 NL and 20 AD subjects (training sets) were chosen at random and a standard scaled subprofile modeling (SSM) analysis was performed to identify AD-related metabolic pattern (ADRP) thus producing 1,000 ADRPs. Each ADRP was defined as the principal component (PC) with the highest discriminative power out of the first 5 PCs [1]. The group-discriminating threshold for ADRP scores was determined based on those sets of scores which exhibited the highest sensitivity × specificity in each training set. The subsequent ADRP generated was then applied to the testing set consisting of the remaining subjects (91 NC and 74 AD) who were not included in the training set.

Machine Voting Score for Alzheimer's Disease (MVAD)

Using the pre-processed ADNI images, random NL (n=20) and AD (n=20) images were selected for incorporation into a training set while accounting for differences in age or sex to create an ADRP with the best AD-related pattern based on the PC with the optimal group discrimination (highest subject scores). After repeating the iteration 1,000 times, the AUC for each individual ADRP obtained was examined to determine the optimal ADRP score threshold which best group discrimination based on sensitivity and specificity.

Many of the subjects whose data were used in this study were on some form of palliative cholinesterase inhibitor medication (AChEI) such as donepezil, memantine, galantamine or a combination thereof. Within the ADNI cohort, there were a total of 75 AD subjects who were on an AChEI, as well as a total of 105 MCI subjects who were medicated. In the HSC cohort, 19 AD and 5 MCI subjects were medicated at the time of PET scanning. To rule out the role of medication as a possible confounding factor in pattern generation and subsequent testing set application of the pattern, the effect of medication within the AD group of the ADNI cohort (which was used to form part of the training set) was examined by comparing the MVADs of those subjects who had been medicated to those of subjects who had not been medicated.

Statistical Analysis

Data analyses used in the generation of the ADRP on randomly selected ADNI AD and NL subjects were carried out using ROC analyses to compute the related AUC for specificity and sensitivity, and subject scores compared using a One-Way Analysis of Variance (ANOVA) or Independent Sample T-Test. The combination of PCs which yielded the highest AUC and thus the highest sensitivity and specificity was chosen as the pattern which was prospectively applied to the various testing sets analyzed during the course of this study.

Figure 5

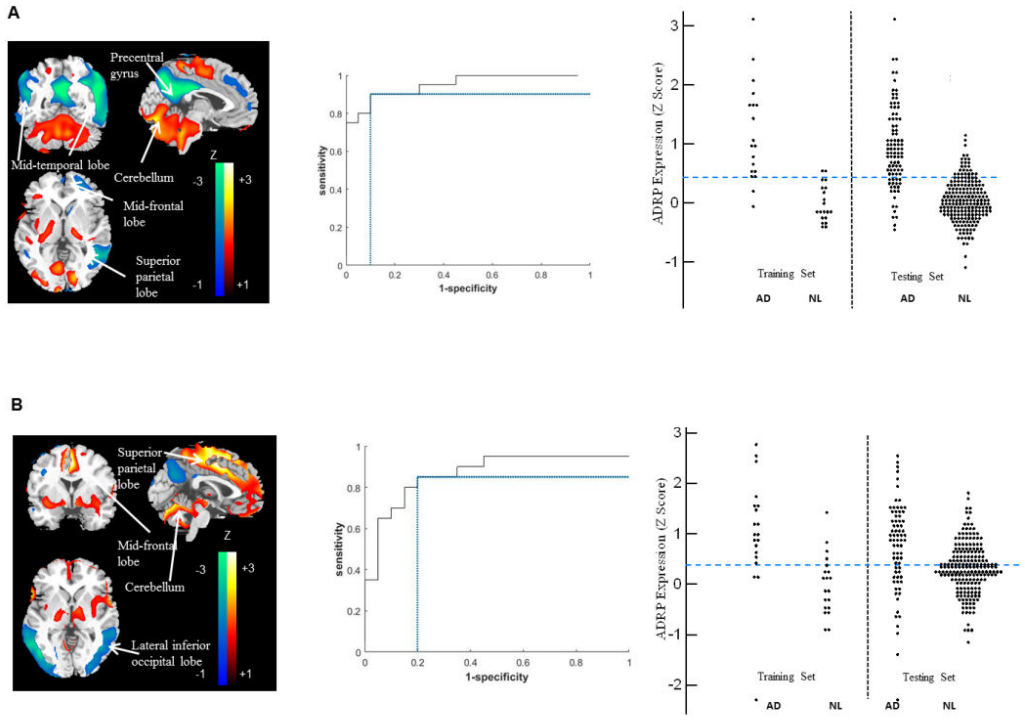

Figure 5: Different ADRPs derived from different training sets A. Sample ADRP with *favorable* performance is visualized. ADRP pattern is in line with prior literature [63, 64] with relative hypometabolism evident within the mid-frontal region, mid- temporal lobes, precentral gyrus, inferior temporal regions, as well as the inferior temporal and superior parietal lobes (*left*). Very good area-under-the-curve (AUC = 0.95) is observed in the receiver-operating curve with 90% sensitivity and 90% specificity (*middle*) with the optimal ADRP score for discriminating groups (z-scored ADRP expression threshold=0.43; blue dashed

lines) in the training set. Significant group discrimination is achieved in both training ($t(19)=5.45$, $p<0.001$) and testing ($t(274)=14.3$, $p<0.001$) sets (*right*). **B.** A sample ADRP with *unfavorable* performance is visualized. ADRP pattern is relatively in line with prior literature but less so than the sample used in top panel with lack of hypometabolism within the anterior cingulate (*left*). Relatively good area-under-the-curve is observed (AUC=0.85) with 85% sensitivity and 80% specificity (*middle*) with the optimal ADRP score for discriminating groups ($z=0.38$; blue dashed lines) in the training set. Significant group discrimination is achieved in the training set ($t(19)=3.724$, $p=<0.001$) but its performance was relatively reduced in the testing set ($t(274)=5.316$, $p<0.001$) (*right*).

As a result of machine voting, each subject was assigned a democratic machine voting score (MVAD) which represented the degree to which an individual expressed the ADRP pattern during disease/group classification. This subject score was utilized during the ANOVA, with medication effect being a confounding factor which was accounted for. MMSE score and age were selected covariates.

To investigate the effect of confounding factors such as age, gender, MMSE score and patient medication status, within-group and inter-group One-Way Analysis of Variance (ANOVA) analyses were conducted. Pearson Correlation analyses were conducted to investigate what relationship, if any may have existed

between MVAD score and age/gender in the HSC cohort. In addition, independent T-tests were carried out against the HSC-MCI group to investigate the effect, if any, of patient age and MMSE score on MVAD. All statistical analysis was performed using IBM SPSS Statistics version 24 and Systat Version 13.1.

6. Results

Construction of 1,000 ADRP-based voting machines

SSM/PCA was used to generate an ADRP with a training set of 20 AD patients with 20 age- and sex-matched healthy normal controls (NL), randomly selected from 94 AD and 111 NL (who stayed normal for at least 3 years) from the ADNI database (Table 1). One thousand ADRPs were constructed with the randomly selected training sets. In each iteration, the rest of the subjects (74 AD and 91 NL) served as a testing set. For visualization purposes, the 1,000 permuted ADRPs were z-scored with respect to the whole brain region weights, then averaged (**Figure 6**). This averaged pattern revealed a well-characterized AD-like distribution [65] of hypometabolism present within the medial frontal lobes, the temporal lobes, and the cingulum (posterior and anterior) and occipital lobes. Relative hypermetabolism was observed in the somatosensory association areas of the parietal lobes, thalamus and cerebellum. Our findings echo those observed in the previously identified ADRP pattern [6].

Figure 6

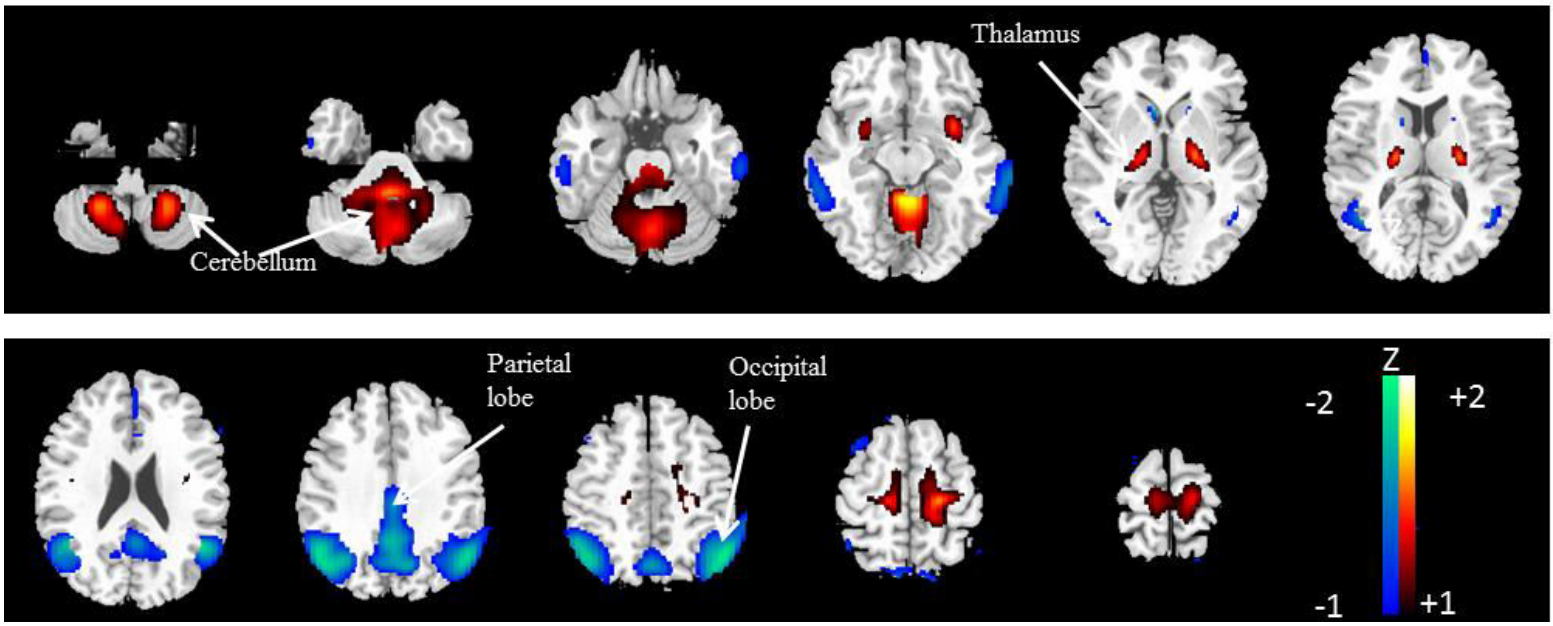

Figure 6: Average of 1,000 ADRPs that consist of the results provided by the 1,000 individual ADRP voting machines. Pattern depicts regions of relative hypometabolism (blue-green) in the bilateral temporal and occipital lobes and the frontal lobes and hypermetabolism (red-yellow) in the cerebellum and medial motor association and Broca's areas[66].

The area-under-the-curve (AUC) in a receiver-operating-characteristic (ROC) plot can serve as an indicator of how well an ADRP allocates subjects to AD vs. NL groups [17]. Although high AUC has been generally observed across the 1,000 permuted ADRPs (0.817±0.059), the need for the use of a voting method afforded to us through machine voting arose due to non-negligible variation in its

performance in the testing sets (AUC: 0.782±0.066, sensitivity: 0.671±0.141, specificity: 0.741±0.141). The final performance indicator values (i.e., AUC, sensitivity and specificity) obtained are dependent on a number of unknown factors including clinical misdiagnosis [67], and the resulting patterns' topographies may significantly vary from each other.

A weak but significant correlation was identified between 1,000 AUCs of the training set and their corresponding AUCs of the testing set (r^2=0.139, $p<0.001$). The AUCs were significantly higher if the permuted ADRP was based on more dominant principal components (PC) (training set: $F(4,995)=9.01$, $p<0.001$; testing set: $F(4,995)=10.76$, $p<0.001$;**Figure 7**).

Figure 7

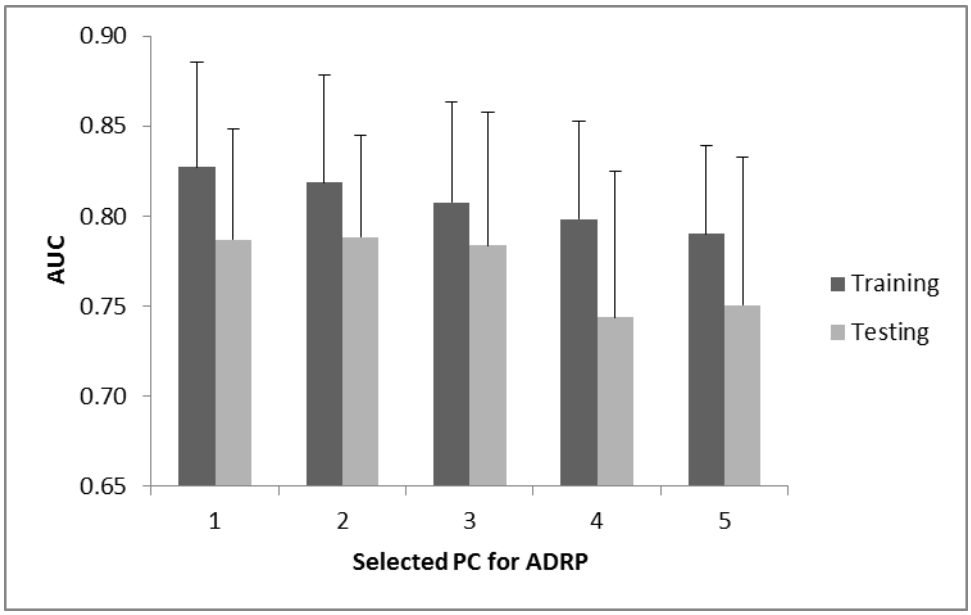

Figure 7: In each of 1,000 permutations, ADRP was selected among the first 5 PCs that produced the best group discrimination by student t-test [17]. In the majority of cases, one of the first 3 PCs were selected (PC1: 466, PC2: 275, PC3: 132, PC4: 76, PC5: 51). The AUC was significantly different across the selected PCs in the training sets ($F(4,995)=9.01$, $p<0.001$) and testing sets ($F(4,995)=10.76$, $p<0.001$). Nevertheless, the post-hoc Bonferroni tests revealed that there was no significant difference in AUCs between ADRPs selected from PC1 and PC2 in both training and testing sets ($p>0.5$) while PC4-5's AUCs were lower than PC1 ($p<0.002$).

Indeed, across the 1,000 permuted ADRP, topographical similarity test [68] yielded a moderate level of cross-correlation (r^2=0.261±0.220). In other words, not all ADRPs are topographically identical, suggesting the existence of multiple spatially distinct metabolic patterns that differentiate AD vs. NL (cf. Brain metabolism in Parkinson's disease is characterized by at least five different spatially distinct pattern that are separately associated with rigidity/akinesia [69], tremor [70], cognition [71], normal movement [72] and placebo effects [73]. Therefore, to accommodate the results of different pattern-based decisions, and thus producing a quantitative result that makes use of the most stable disease-distinguishing characteristics, a voting method was developed.

In each training set, the optimal threshold for ADRP scores were determined to have the highest sensitivity × specificity (i.e., best group discrimination) so that each ADRP could vote a subject to be either AD or NL accordingly. The proportion of positive votes (toward AD) was calculated for each subject. The voting results used for subjects in training sets were discarded, thus the total votes for each subject was less than 1,000 (AD: 787 ± 20, NL: 820 ± 20). The majority of AD (n=72 out of 94) received higher proportion of positive AD votes (machine voting for Alzheimer's disease scores; MVAD > 50%) while the majority of NL (n=89 out of 111) received a lower proportion of AD votes (MVAD < 50%) (**Figure 8**). At 50% MVAD-threshold, the projected sensitivity is 0.76 and the

specificity is 0.81. Since post-mortem confirmation is not available at the moment, 0.7-0.9 sensitivity and 0.4-0.7 specificity is the highest performance that one can achieve with the clinical follow-up diagnosis as a gold standard [62].

Figure 8

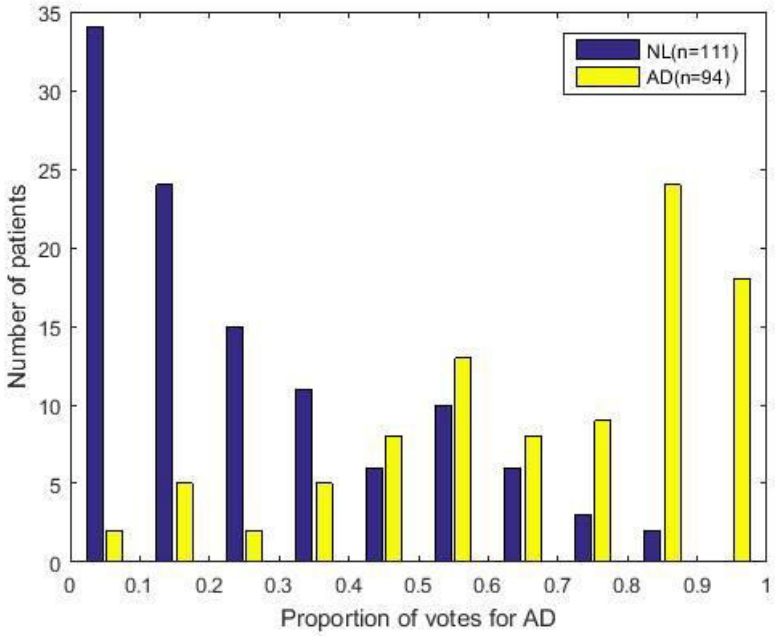

Figure 8: Histogram of Machine Voting Score for Alzheimer's Disease (MVAD) of Alzheimer's disease (AD) and normal control subjects (NL) from ADNI database. The results of 1,000 ADRP vote proportions for NL and AD subjects were depicted. It should be noted that the MVAD was only considered when each subject was classified as testing set thus the actual number of votes that each subject received is less than 1,000. Trend clearly depicts discriminative power of

MVAD with the majority of NL (72 out of 111) received mostly negative votes (<30%). Likewise, the majority of AD patients (61 out of 94) received mostly positive votes (>70%).

Identifying prodromal AD

The assigned voting score (MVAD) proved to be a tool with modest predictive power and wielded fairly good predictive accuracy in distinguishing between those subjects with MCI who converted to AD (prodromal AD) from those who remained stable for more than 3 years (stable MCI) (**Figure 9**). The 32 out of 55 prodromal AD subjects were classified as exhibiting AD-like glucose metabolic patterns, receiving a higher proportion of positive votes (MVAD > 50%), while 142 out of 186 stable MCI subjects received a lower proportion of AD votes (MVAD < 50%). At a 50% voting threshold identical to the one utilized in distinguishing NL from AD, a sensitivity of 0.58 was attained, while specificity rested at a modest 0.76.

Figure 9

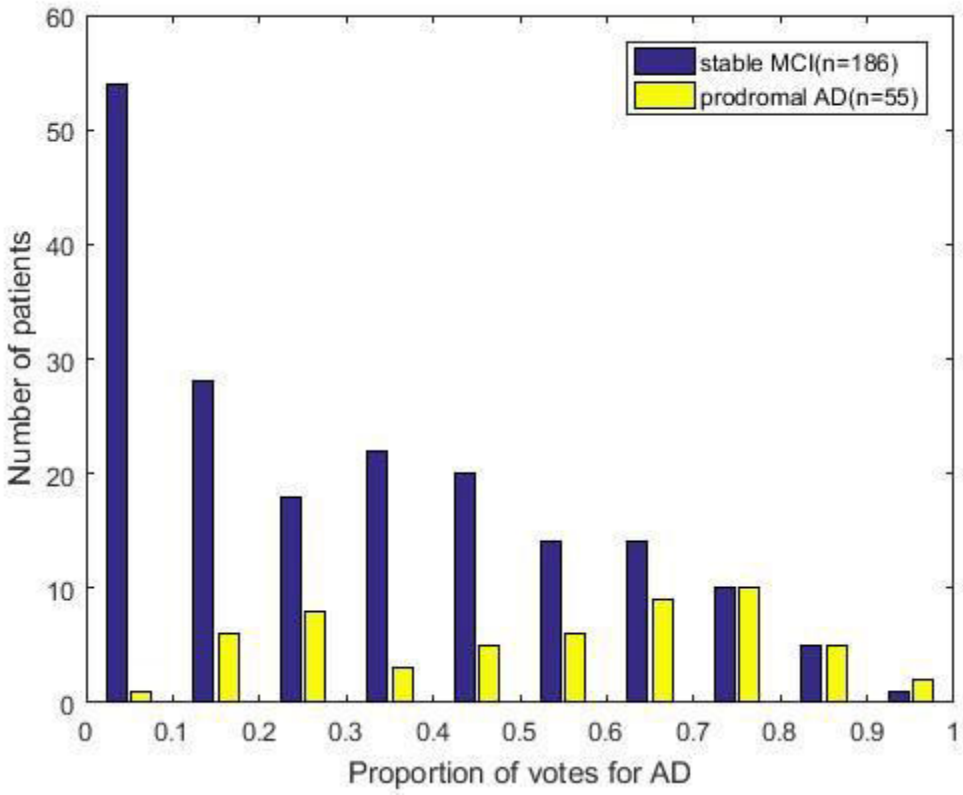

Figure 9: Histogram of Machine Voting Score for Alzheimer's Disease (MVAD) of prodromal Alzheimer's disease (AD) and stable mild cognitive impairment (MCI) from ADNI database. MCI patients were scanned with FDG-PET at baseline and followed up for clinical diagnosis. The MCI patients who developed AD in the next 3 years were classified as prodromal AD. For stable MCI, only the patients who had not developed any forms of dementia for the next 3 years were included. Trend depicts moderate predictive power of MVAD with the majority of stable MCI (101 out of 186) received mostly negative votes (<30%). 17 out of 55 prodromal AD received mostly positive votes (>70%).

Potential Confounding Factors

Potential confounding factors for MVAD included medication status, different PET scanner types, as well as patient age, sex and MMSE score. In order to rule out the possible role of medication as a confounding factor, the effect of medication within the AD, prodromal AD, stable MCI and NL group of the ADNI cohort was examined by comparing the MVADs of those subjects who had been medicated to those of subjects who had not been medicated. No significant effect of medication was found ($p>0.238$). A similar analysis was conducted on the scores assigned by the pattern to the MCI converters in the ADNI cohort in contrast to non-converters. This analysis, too yielded results which emphasized that the ADRP is unaffected by the medication status of the patient being studied ($t= 1.153$).

SSM/PCA is known to be insensitive to different scanner types and pre-processing procedures [74]. Thus, as expected, no significant differences in MVAD were observed across the different scanner type ($p>0.301$). Neither age ($p>0.083$), sex ($p>0.180$) nor MMSE ($p>0.061$) was associated with MVAD scores ($r^2=0.291\pm0.287$) within each group.

Translational Utility Demonstration

The retrospective chart review conducted at our PET center identified 83 patients with undetermined diagnosis referred for brain FDG-PET from our local memory clinic. Assuming clinical follow-up diagnosis is the gold standard, the proposed voting method classified the majority of patients who were later diagnosed with dementia as AD (**Figure 10**). At 50% MVAD-threshold, 15 of 20 AD, 14 of 16 DLB, 2 of 4 FTD, 4 of 5 VaD, 6 of 18 stable MCI patients (follow up duration 58.2 months ±17.9) were voted to have AD.

Figure 10

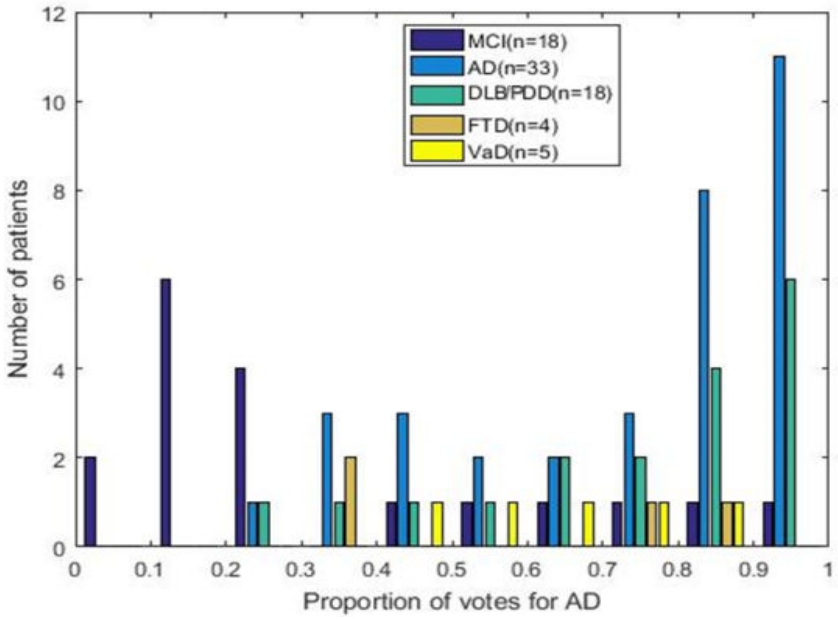

Figure 10: Histogram of Machine Voting Score for Alzheimer's disease (MVAD) of Health Science Centre (HSC) cohort. Patients from local memory clinic were referred for FDG-PET scan due to undetermined clinical diagnosis and followed up for clinical diagnosis. 60 patients developed dementia, 33 AD, 18 DLB/PDD, 4 FTD and 5 VaD. For stable MCI (n=18), only patients who had not developed any forms of dementia for the next 3 years were included. Trend depicts strong predictive power of MVAD with the majority of stable MCI (12 out of 18) receiving mostly negative votes (<30%). %). Likewise, the majority of AD patients (22 out of 33) received mostly positive votes (>70%). Interestingly, the majority of DLB/PDD patients (12 out of 18) also received mostly positive votes (>70%). Albeit the low sample size, none of the FTD nor VaD patients received mostly negative votes (<30%).

7. Discussion

The hallmark of the proposed method (i.e., MVAD) is that we automated brain FDG PET readings and produced unbiased estimates of probability of AD diagnosis. The current specificity and sensitivity of clinical PET readings in diagnosing AD rest at a reported 59-87% and 44-75% respectively [16], whereas our method can differentiate between AD and normal subjects with a sensitivity of 76.6% and a specificity of 81.1%. The moderate level of false positives suggests that the potential role of MVAD in early prediction (i.e., considering the high incidence rate of AD in the elderly population), normal subjects with high MVAD may have developed AD if a longer follow-up was available, which is supported by the MCI data. The MVAD was also able to, with modest accuracy, classify MCI subjects who later developed AD (prodromal AD) and differentiate them from those who did not develop AD within the 3 years of follow-up period (stable MCI). On the other hand, the non-negligible false negatives suggest some potential misdiagnosis in the clinical data that is not post-mortem confirmed (see below for detailed discussion).

The methods proposed in this paper provide a useful classification tool which can differentiate between subjects with MCI who are at risk of developing AD from those who remain stable. If these subjects can be isolated, this presents an opportunity for the development of preventative therapies which could be targeted

to this demographic of prodromal AD. Not only does this have the potential to improve the prognosis for this subset of patients, it could also decrease the overall social and economic burden of AD through early diagnosis of prodromal AD. Although there is currently no approved treatment for MCI, there are a number of therapeutic treatments that are in the research and development pipeline, such as the use of intranasal delivery of insulin as a therapy to counteract the cognitive symptoms of AD which has thus far proven to be successful in ongoing clinical trial [75]. Other ongoing trials include the use of novel therapies such as nicotine [76] and anti-hypertensive drug treatments [77] for the amelioration of MCI.

Overall, the averaged ADRP topography (note that this averaging was only used for visualization purposes) was able to pinpoint relative hypometabolism in key brain regions commonly affected by AD: the occipital, frontal and temporal lobes and the cingulum [78]. Nevertheless, only a moderate level of topographical similarity for the whole-brain was observed across the permuted ADRPs, potentially due to the existence of multiple spatial patterns that can separately characterize AD-like brains. Therefore, the non-consensus results of 1,000 votes can be considered as a "minority opinion" using different ADRPs in clinic application. For example, a patient A's MVAD score of 25% can be interpreted as asking for a diagnostic opinion from 1,000 individual neuroradiologists with different training background and 25% of them classified the patient A's FDG-PET

image as AD-like. The proposed method can be implemented in the PET clinic to streamline its operation, e.g., physicians may pay more attention to those cases with a moderate MVAD scores (30-70%) than those with >70% or <30% of whom are more likely to be AD or normal (or stable MCI), respectively. The resulting MVAD score may be included in the nuclear medicine physician's report to the referring physicians who ultimately decide on clinical diagnosis and how to treat the patients. It should be noted that MVAD is derived solely depending on automated FDG-PET reading and independent from other relevant factors such as age, sex, cognitive performance, genetics and medication status, thus it only adds independent and unbiased information to a patient file.

Indeed, no covariates that were considered (i.e., age, sex, medication, MMSE and scanner types) showed significant relationships with MVAD in AD and prodromal AD. However, stable MCI patients who were on medication showed higher MVAD scores. Thus, it was postulated that had there been a longer follow-up period, perhaps some stable MCI subjects would have converted to AD, and classified as prodromal AD. Likewise, age was not correlated with MVAD in AD and prodromal AD, but a significant, albeit weak (r^2<0.14), positive relationship was observed in NL and stable MCI. This may have been due to the fact that once a subject had converted to AD or had prodromal AD, the factor of age may have begun to play a reduced role in the disease progression as the

individual had already developed AD and was no longer simply at risk of conversion. One of the most interesting but controversial finding was the higher MVAD score in male vs. female in NL and stable MCI, which is in direct contradiction of the consensus that female gender provides a higher propensity for the development of AD [79]. One potential explanation is that assuming males have higher "resistance" to AD development, these male individuals with higher MVAD may have developed a compensatory mechanism that suppresses progression to AD despite of their AD-like brain metabolic pattern. In this regard, it is of the highest interest to longitudinally investigate the stable MCI patients with high MVAD, rather than the prodromal AD, in an effort to identify novel therapeutic targets for boosting resistance to AD pathology.

Limitations

A longer available follow-up period for both ADNI and HSC subjects could have proved to be highly beneficial from a statistical standpoint. Incorporating a larger number of subjects with a follow-up period exceeding 36 months could allow for the clinical follow-up of a potentially greater proportion of converting (prodromal AD) subjects. This would essentially increase the demonstrated accuracy of the method without adversely affecting pattern topography.

Nevertheless, unlike most other multivariate pattern analysis techniques, it should be noted that SSM/PCA's resulting principal component topography is not affected by false group designation [17].

It must be noted that the MVAD is only designed for "diagnosis" and is therefore not designed to convey any information about disease progression. It could, however, prove to be highly beneficial to analyze the existing AD-patient longitudinal data provided by the ADNI.

The potential factors that may have influenced MVAD such as sex, age, MMSE, scanner types and medication status have shown to be not interacting with MVAD results. However, these analyses were carried out cross-sectionally. Thus test-retest studies, intervention studies, as well as longitudinal observation studies are warranted.

Future Directions and Potential Translation

The robust performance of MVAD classification of AD vs. stable MCI patients recruited from our community-based memory clinic demonstrates its immediate translational value. It should be noted that all HSC subjects were referred for PET scanning due to difficulty in clinical-only diagnosis, thus there may have been a high chance of dementia comorbidity within these groups of patients. Interestingly, most patients with other forms of dementia (i.e., clinically

determined during the follow-up period) also show non-negligible MVAD scores. The DLB/PDD patients, especially, showed identical levels of MVAD to AD patients. This came as no surprise since DLB/PDD and AD often present with very similar clinical symptoms and neuropathology. Amyloid deposits and tau protein accumulation are commonly observed in patients with DLB, and it has been well established that these AD-related pathologies are also linked to the cognitive deficits that occur in DLB patients [80]. The similar neurodegenerative etiology of the two is also often reflected in FDG-PET scans [81]. The hypometabolic pattern observed in DLB is highly congruent with and can be easily superimposed onto that observed in AD patients with the only region exhibiting variation between the two being the occipital lobe [82]. This clinical overlap makes the two diseases fairly difficult to distinguish and accurate differential diagnosis between AD and DLB remains a popular arena of neurodegenerative disease research, and it is warranted that an additional step be taken for differential diagnosis, e.g., Parkinson's disease-related metabolic pattern expression may be examined in these patients [83]. Other PET/SPECT radiotracers that target the dopaminergic [84] system or tau [85] have shown promising results for differentiating DLB from AD.

FTD is the third most prevalent form of dementia [86]. It involves the aggregation of ubiquitin and DNA binding-protein inclusions [87] and can be identified by hypometabolic frontal and anterior temporal lobes [88]. Of the 4

HSC-FTD subjects studied, there was an even split among them with 2 patients exhibiting moderate level of MVAD scores (30-40%) and 2 exhibiting high level of MVAD scores (70-80%). Likewise, none of the HSC-VaD patients exhibited MVAD scores <30%. Of the 5 subjects available for study, 2 expressed AD pathology with >90% certainty per the voting machine. The other 3 subjects expressed the pattern with an array votes numbering between 36% and 78%, again underlining the heterogeneity present within the disease [89]. The unavailability of post-mortem diagnoses and small sample size prevent any definite conclusions, but it is noteworthy to report that none of the FTD and VaD patients were at a low level of MVAD (<30%). This therefore warrants close inspection by nuclear medicine physicians and follow-ups if done in a clinical setting.

8. Conclusion

Our method was able to provide an objective diagnostic approach for classifying individual subjects into disease groups based on quantifiable expression of the characteristic disease (AD) pattern. Conferring an accurate diagnosis of AD continues to present several challenges, and with the prognosis as poor as it is, the need for the development of diagnostic techniques that can predict the probability of developing AD from the stage of MCI remains ever-present [90]. Accurate screening and diagnosis at an early stage will help patients and caregivers by

providing a better chance of benefiting from treatment, relief from anxiety about unknown problems, more time to plan for the future and early access to psychosocial education for both patients and caregivers [22]. In addition, early identification of at-risk individuals will be extremely useful for clinical trials of disease modifying or protective therapies, which should be specifically effective when therapeutic intervention occurs in the early phases of the disease.

9. References

[1] P. Spetsieris, Y. Ma, S. Peng, J.H. Ko, V. Dhawan, C.C. Tang, D. Eidelberg, Identification of Disease-related Spatial Covariance Patterns using Neuroimaging Data, Jove-Journal of Visualized Experiments, DOI 10.3791/50319(2013).

[2] J. McConathy, Y.I. Sheline, Imaging Biomarkers Associated With Cognitive Decline: A Review, Biol Psychiatry, DOI 10.1016/j.biopsych.2014.08.024(2014).

[3] K. Ishii, A.K. Kono, H. Sasaki, N. Miyamoto, T. Fukuda, S. Sakamoto, E. Mori, Fully automatic diagnostic system for early- and late-onset mild Alzheimer's disease using FDG PET and 3D-SSP, European Journal of Nuclear Medicine and Molecular Imaging, 33 (2006) 575-583.

[4] C. Habeck, Y. Stern, I. Alzheimer's Disease Neuroimaging, Multivariate data analysis for neuroimaging data: overview and application to Alzheimer's disease, Cell Biochem Biophys, 58 (2010) 53-67.

[5] S. Morbelli, D. Arnaldi, S. Capitanio, A. Picco, A. Buschiazzo, F. Nobili, Resting metabolic connectivity in Alzheimer's disease, Clinical and Translational Imaging, 1 (2013) 271-278.

[6] P.J. Mattis, M. Niethammer, W. Sako, C.C. Tang, A. Nazem, M.L. Gordon, V. Brandt, V. Dhawan, D. Eidelberg, Distinct brain networks underlie cognitive

dysfunction in Parkinson and Alzheimer diseases, Neurology, 87 (2016) 1925-1933.

[7] M.R. Brier, J.B. Thomas, B.M. Ances, Network Dysfunction in Alzheimer's Disease: Refining the Disconnection Hypothesis, Brain Connectivity, 4 (2014) 299-311.

[8] W.E. Klunk, H. Engler, A. Nordberg, Y. Wang, G. Blomqvist, D.P. Holt, M. Bergstrom, I. Savitcheva, G.F. Huang, S. Estrada, B. Ausen, M.L. Debnath, J. Barletta, J.C. Price, J. Sandell, B.J. Lopresti, A. Wall, P. Koivisto, G. Antoni, C.A. Mathis, B. Langstrom, Imaging brain amyloid in Alzheimer's disease with Pittsburgh Compound-B, Ann Neurol, 55 (2004) 306-319.

[9] Y. Ma, S. Zhang, J. Li, D.M. Zheng, Y. Guo, J. Feng, W.D. Ren, Predictive accuracy of amyloid imaging for progression from mild cognitive impairment to Alzheimer disease with different lengths of follow-up: a systematic review, Medicine, 93 (2014) e150.

[10] M.J. Pontecorvo, M.A. Mintun, PET amyloid imaging as a tool for early diagnosis and identifying patients at risk for progression to Alzheimer's disease, Alzheimer's research & therapy, 3 (2011) 11.

[11] W. Jagust, Time for tau, Brain, 137 (2014) 1570-1571.

[12] S. Kannan, B. Balakrishnan, O. Muzik, R. Romero, D. Chugani, PET Imaging of Neuroinflammation, Journal of child neurology, 24 (2009) 10.1177/0883073809338063.

[13] A.J. Saykin, K.K. Yoder, S.L. Risacher, T.R. MaGee, B.C. McDonald, Q.-H. Zheng, M. Wang, B.H. Mock, L. Shen, J.D. West, J.W. Fletcher, M.R. Farlow, G.D. Hutchins, Neuroinflammation and amyloid deposition: Concurrent [11C]PBR28 and [11C]PIB PET imaging in patients with Alzheimer's disease, mild cognitive impairment, and older adults with cognitive complaints, Alzheimer's & Dementia, 6 (2010) S3-S4.

[14] P. Rosenberg, C. Endres, C. Lyketsos, J. Coughlin, M. Kassiou, M. Pomper, Quantifying translocator protein (TSPO) in Alzheimer's disease and cognitively healthy older persons with 11C-DPA-713 PET imaging, Alzheimer's & Dementia, 7 (2011) S725.

[15] I. Suridjan, R. Pablo, B. Pollock, A. Voineskos, A. Wilson, H. Sylvain, R. Mizrahi, Mapping neuroinflammation in vivo in healthy aging and Alzheimer's disease: A PET study using a novel translocator protein 18kDA (TSPO) radioligand, [18F]-FEPPA, Alzheimer's & Dementia, 8 (2012) P693.

[16] J.L. Shaffer, J.R. Petrella, F.C. Sheldon, K.R. Choudhury, V.D. Calhoun, R.E. Coleman, P.M. Doraiswamy, I. Alzheimer's Disease Neuroimaging, Predicting cognitive decline in subjects at risk for Alzheimer disease by using combined

cerebrospinal fluid, MR imaging, and PET biomarkers, Radiology, 266 (2013) 583-591.

[17] P. Spetsieris, Y. Ma, S. Peng, J.H. Ko, V. Dhawan, C.C. Tang, D. Eidelberg, Identification of Disease-related Spatial Covariance Patterns using Neuroimaging Data, J Vis Exp, DOI 10.3791/50319(2013).

[18] C.C. Tang, K.L. Poston, T. Eckert, A. Feigin, S. Frucht, M. Gudesblatt, V. Dhawan, M. Lesser, J.P. Vonsattel, S. Fahn, D. Eidelberg, Differential diagnosis of parkinsonism: a metabolic imaging study using pattern analysis, Lancet Neurol, 9 (2010) 149-158.

[19] F. Holtbernd, J.F. Gagnon, R.B. Postuma, Y. Ma, C.C. Tang, A. Feigin, V. Dhawan, M. Vendette, J.P. Soucy, D. Eidelberg, J. Montplaisir, Abnormal metabolic network activity in REM sleep behavior disorder, NEUROLOGY NEUROLOGY, DOI 10.1212/wnl.0000000000000130(2014).

[20] M. Niethammer, C.C. Tang, A. Feigin, P.J. Allen, L. Heinen, S. Hellwig, F. Amtage, E. Hanspal, J.P. Vonsattel, K.L. Poston, P.T. Meyer, K.L. Leenders, D. Eidelberg, A disease-specific metabolic brain network associated with corticobasal degeneration, Brain, 137 (2014) 3036-3046.

[21] A global assessment of dementia, now and in the future, Lancet, 386 (2015) 931-931.

[22] M. Prince, R. Bryce, C. Ferri, World Alzheimer report 2011: the benefits of early diagnosis and intervention., Alzheimer's Disease International (ADI), London (UK), 2011, pp. 68.

[23] C.X. Qiu, D. De Ronchi, L. Fratiglioni, The epidemiology of the dementias: an update, Current Opinion in Psychiatry, 20 (2007) 380-385.

[24] K.M. Rodrigue, K.M. Kennedy, D.C. Park, Beta-Amyloid Deposition and the Aging Brain, Neuropsychology Review, 19 (2009) 436-450.

[25] M. Ahuja, M. Buabeid, E. Abdel-Rahman, M. Majrashi, K. Parameshwaran, R. Amin, S. Ramesh, K. Thiruchelvan, S. Pondugula, V. Suppiramaniam, M. Dhanasekaran, Immunological alteration & toxic molecular inductions leading to cognitive impairment & neurotoxicity in transgenic mouse model of Alzheimer's disease, Life Sciences, 177 (2017) 49-59.

[26] H. Amieva, M. Le Goff, X. Millet, J.M. Orgogozo, K. Peres, P. Barberger-Gateau, H. Jacqmin-Gadda, J.F. Dartigues, Prodromal Alzheimer's Disease: Successive Emergence of the Clinical Symptoms, Annals of Neurology, 64 (2008) 492-498.

[27] L. Mosconi, V. Berti, L. Glodzik, A. Pupi, S. De Santi, M.J. de Leon, Pre-Clinical Detection of Alzheimer's Disease Using FDG-PET, with or without Amyloid Imaging, Journal of Alzheimers Disease, 20 (2010) 843-854.

[28] R.T. Owen, MEMANTINE AND DONEPEZIL: A FIXED DRUG COMBINATION FOR THE TREATMENT OF MODERATE TO SEVERE ALZHEIMER'S DEMENTIA, Drugs of Today, 52 (2016) 239-248.

[29] M.W. Weiner, D.P. Veitch, P.S. Aisen, L.A. Beckett, N.J. Cairns, R.C. Green, D. Harvey, C.R. Jack, W. Jagust, J.C. Morris, R.C. Petersen, J. Salazar, A.J. Saykin, L.M. Shaw, A.W. Toga, J.Q. Trojanowski, I. Alzheimer's Dis Neuroimaging, The Alzheimer's Disease Neuroimaging Initiative 3: Continued innovation for clinical trial improvement, Alzheimers & Dementia, 13 (2017) 561-571.

[30] R.C. Petersen, Early Diagnosis of Alzheimer's Disease: Is MCI Too Late?, Current Alzheimer research, 6 (2009) 324-330.

[31] M.P. Murphy, H. LeVine, Alzheimer's Disease and the β-Amyloid Peptide, Journal of Alzheimer's disease : JAD, 19 (2010) 311.

[32] K. Iqbal, F. Liu, C.-X. Gong, I. Grundke-Iqbal, Tau in Alzheimer Disease and Related Tauopathies, Current Alzheimer research, 7 (2010) 656-664.

[33] M.R. Sabuncu, R.S. Desikan, J. Sepulcre, B.T.T. Yeo, H. Liu, N.J. Schmansky, M. Reuter, M.W. Weiner, R.L. Buckner, R.A. Sperling, B. Fischl, The Dynamics of Cortical and Hippocampal Atrophy in Alzheimer Disease, Archives of neurology, 68 (2011) 1040-1048.

[34] M.T. Heneka, M.J. Carson, J.E. Khoury, G.E. Landreth, F. Brosseron, D.L. Feinstein, A.H. Jacobs, T. Wyss-Coray, J. Vitorica, R.M. Ransohoff, K. Herrup, S.A. Frautschy, B. Finsen, G.C. Brown, A. Verkhratsky, K. Yamanaka, J. Koistinaho, E. Latz, A. Halle, G.C. Petzold, T. Town, D. Morgan, M.L. Shinohara, V.H. Perry, C. Holmes, N.G. Bazan, D.J. Brooks, S. Hunot, B. Joseph, N. Deigendesch, O. Garaschuk, E. Boddeke, C.A. Dinarello, J.C. Breitner, G.M. Cole, D.T. Golenbock, M.P. Kummer, Neuroinflammation in Alzheimer's disease, The Lancet Neurology, 14 388-405.

[35] J.Y. Wang, L.L. Wen, Y.N. Huang, Y.T. Chen, M.C. Ku, Dual effects of antioxidants in neurodegeneration: Direct neuroprotection against oxidative stress and indirect protection via suppression of glia-mediated inflammation, Current Pharmaceutical Design, 12 (2006) 3521-3533.

[36] C. Reitz, C. Brayne, R. Mayeux, Epidemiology of Alzheimer disease, Nat Rev Neurol, 7 (2011) 137-152.

[37] R. Mayeux, Y. Stern, Epidemiology of Alzheimer Disease, Cold Spring Harbor perspectives in medicine, 2 (2012) 10.1101/cshperspect.a006239 a006239.

[38] M.F. Mendez, Early-Onset Alzheimer Disease, Neurologic Clinics, 35 (2017) 263-281.

[39] A. Antonell, M. Balasa, R. Oliva, A. Lladó, B. Bosch, N. Fabregat, J. Fortea, J.L. Molinuevo, R. Sánchez-Valle, A novel PSEN1 gene mutation (L235R)

associated with familial early-onset Alzheimer's disease, Neuroscience Letters, 496 (2011) 40-42.

[40] G.M. McKhann, D.S. Knopman, H. Chertkow, B.T. Hyman, C.R. Jack, C.H. Kawas, W.E. Klunk, W.J. Koroshetz, J.J. Manly, R. Mayeux, R.C. Mohs, J.C. Morris, M.N. Rossor, P. Scheltens, M.C. Carrillo, B. Thies, S. Weintraub, C.H. Phelps, The diagnosis of dementia due to Alzheimer's disease: Recommendations from the National Institute on Aging-Alzheimer's Association workgroups on diagnostic guidelines for Alzheimer's disease, Alzheimer's & dementia : the journal of the Alzheimer's Association, 7 (2011) 263-269.

[41] A.D. Benson, M.J. Slavin, T.-T. Tran, J.R. Petrella, P.M. Doraiswamy, Screening for Early Alzheimer's Disease: Is There Still a Role for the Mini-Mental State Examination?, Primary Care Companion to The Journal of Clinical Psychiatry, 7 (2005) 62-69.

[42] Y. Zhou, F. Ortiz, C. Nuñez, D. Elashoff, E. Woo, L.G. Apostolova, S. Wolf, M. Casado, N. Caceres, H. Panchal, J.M. Ringman, Use of the MoCA in Detecting Early Alzheimer's Disease in a Spanish-Speaking Population with Varied Levels of Education, Dementia and Geriatric Cognitive Disorders EXTRA, 5 (2015) 85-95.

[43] M.M. Williams, C.M. Roe, J.C. Morris, Stability of the Clinical Dementia Rating: 1979–2007, Archives of neurology, 66 (2009) 773-777.

[44] L. Mosconi, W.H. Tsui, K. Herholz, A. Pupi, A. Drzezga, G. Lucignani, E.M. Reiman, V. Holthoff, E. Kalbe, S. Sorbi, J. Diehl-Schmid, R. Perneczky, F. Clerici, R. Caselli, B. Beuthien-Baurnann, A. Kurz, S. Minoshima, M.J. de Leon, Multicenter standardized F-18-FDG PET diagnosis of mild cognitive impairment, Alzheimer's disease, and other dementias, Journal of Nuclear Medicine, 49 (2008) 390-398.

[45] A. Moore, C. Patterson, L. Lee, I. Vedel, H. Bergman, D. Canadian Consensus Conference on the, D. Treatment of, Fourth Canadian Consensus Conference on the Diagnosis and Treatment of Dementia: recommendations for family physicians, Canadian family physician Medecin de famille canadien, 60 (2014) 433-438.

[46] A.J. Mitchell, M. Shiri-Feshki, Rate of progression of mild cognitive impairment to dementia--meta-analysis of 41 robust inception cohort studies, Acta Psychiatr Scand, 119 (2009) 252-265.

[47] S. Shipley, B. Kluger, C. Filley, Accuracy of Community-Acquired PET Scans in the Diagnosis of Dementia, Neurology, 78 (2012).

[48] C. Marcus, E. Mena, R.M. Subramaniam, Brain PET in the Diagnosis of Alzheimer's Disease, Clinical nuclear medicine, 39 (2014) e413-e426.

[49] O. Zanetti, S.B. Solerte, F. Cantoni, LIFE EXPECTANCY IN ALZHEIMER'S DISEASE (AD), Archives of Gerontology and Geriatrics, 49 237-243.

[50] R. Cacabelos, Donepezil in Alzheimer’s disease: From conventional trials to pharmacogenetics, Neuropsychiatric Disease and Treatment, 3 (2007) 303-333.

[51] W.J. Deardorff, G.T. Grossberg, A fixed-dose combination of memantine extended-release and donepezil in the treatment of moderate-to-severe Alzheimer's disease, Drug Design Development and Therapy, 10 (2016).

[52] X.L. Zhou, Y.F. Li, X.Z. Shi, C. Ma, An overview on therapeutics attenuating amyloid beta level in Alzheimer's disease: targeting neurotransmission, inflammation, oxidative stress and enhanced cholesterol levels, American Journal of Translational Research, 8 (2016) 246-269.

[53] V.E. Semenov, I.V. Zueva, M.A. Mukhamedyarov, S.V. Lushchekina, A.D. Kharlamova, E.O. Petukhova, A.S. Mikhailov, S.N. Podyachev, L.F. Saifina, K.A. Petrov, O.A. Minnekhanova, V.V. Zobov, E.E. Nikolsky, P. Masson, V.S. Reznik, 6-Methyluracil Derivatives as Bifunctional Acetylcholinesterase Inhibitors for the Treatment of Alzheimer's Disease, Chemmedchem, 10 (2015) 1863-1874.

[54] K.R. Ma, J. McLaurin, alpha-Melanocyte Stimulating Hormone as a Potential Therapy for Alzheimer's Disease, Current Alzheimer Research, 14 (2017) 18-29.

[55] N.G. Faux, C.W. Ritchie, A. Gunn, A. Rembach, A. Tsatsanis, J. Bedo, J. Harrison, L. Lannfelt, K. Blennow, H. Zetterberg, M. Ingelsson, C.L. Masters, R.E. Tanzi, J.L. Cummings, C.M. Herd, A.I. Bush, PBT2 Rapidly Improves Cognition in Alzheimer's Disease: Additional Phase II Analyses, Journal of Alzheimers Disease, 20 (2010) 509-516.

[56] M.W. Weiner, D.P. Veitch, P.S. Aisen, L.A. Beckett, N.J. Cairns, J. Cedarbaum, R.C. Green, D. Harvey, C.R. Jack, W. Jagust, J. Luthman, J.C. Morris, R.C. Petersen, A.J. Saykin, L. Shaw, L. Shen, A. Schwarz, A.W. Toga, J.Q. Trojanowski, 2014 Update of the Alzheimer's Disease Neuroimaging Initiative: A review of papers published since its inception, Alzheimer's & Dementia, 11 (2015) e1-e120.

[57] D. Zhang, D. Shen, Multi-modal multi-task learning for joint prediction of multiple regression and classification variables in Alzheimer's disease, NeuroImage, 59 (2012) 895-907.

[58] T. Tong, K. Gray, Q.Q. Gao, L. Chen, D. Rueckert, I. Alzheimers Dis Neuroimaging, Multi-modal classification of Alzheimer's disease using nonlinear graph fusion, Pattern Recognition, 63 (2017) 171-181.

[59] H.J. Yun, K. Kwak, J.M. Lee, I. Alzheimer's Dis Neuroimaging, Multimodal Discrimination of Alzheimer's Disease Based on Regional Cortical Atrophy and Hypometabolism, Plos One, 10 (2015).

[60] J.L. Hsu, W.C. Hsu, C.C. Chang, K.J. Lin, I.T. Hsiao, Y.C. Fan, C.H. Bai, Everyday cognition scales are related to cognitive function in the early stage of probable Alzheimer's disease and FDG-PET findings, Scientific Reports, 7 (2017).

[61] E.H. Seo, D.Y. Lee, J.M. Lee, J.S. Park, B.K. Sohn, D.S. Lee, Y.M. Choe, J.I. Woo, Whole-brain Functional Networks in Cognitively Normal, Mild Cognitive Impairment, and Alzheimer's Disease, Plos One, 8 (2013).

[62] C.A. de Jager, T.E.M. Honey, J. Birks, G.K. Wilcock, Retrospective evaluation of revised criteria for the diagnosis of Alzheimer's disease using a cohort with post-mortem diagnosis, International Journal of Geriatric Psychiatry, 25 (2010) 988-997.

[63] A. Bakkour, J.C. Morris, D.A. Wolk, B.C. Dickerson, The effects of aging and Alzheimer's disease on cerebral cortical anatomy: Specificity and differential relationships with cognition, Neuroimage, 76 (2013) 332-344.

[64] Y. Chen, D.A. Wolk, J.S.R. Eddin, M. Korczykowski, P.M. Martinez, E.S. Pvlusiek, A.B. Newberg, P. Julin, S.E. Arnold, J.H. Greenberg, J.A. Detre, Voxel-level comparison of arterial spin-labeled perfusion MRI and FDG-PET in Alzheimer disease, Neurology, 77 (2011) 1977-1985.

[65] L. Mosconi, Brain glucose metabolism in the early and specific diagnosis of Alzheimer's disease - FDG-PET studies in MCI and AD, European Journal of Nuclear Medicine and Molecular Imaging, 32 (2005) 486-510.

[66] Y. Chiba, H. Fujishiro, K. Ota, K. Kasanuki, H. Arai, Y. Hirayasu, K. Sato, E. Iseki, Clinical profiles of dementia with Lewy bodies with and without Alzheimer's disease-like hypometabolism, International Journal of Geriatric Psychiatry, 30 (2015) 316-323.

[67] O.M. Doyle, E. Westman, A.F. Marquand, P. Mecocci, B. Vellas, M. Tsolaki, I. Kloszewska, H. Soininen, S. Lovestone, S.C.R. Williams, A. Simmons, A. AddNeuroMed Consortium, Predicting Progression of Alzheimer's Disease Using Ordinal Regression, Plos One, 9 (2014).

[68] J.H. Ko, P. Spetsieris, Y. Ma, V. Dhawan, D. Eidelberg, Quantifying significance of topographical similarities of disease-related brain metabolic patterns, PLoS One, 9 (2014) e88119.

[69] D. Eidelberg, J.R. Moeller, V. Dhawan, P. Spetsieris, S. Takikawa, T. Ishikawa, T. Chaly, W. Robeson, D. Margouleff, S. Przedborski, The metabolic topography of parkinsonism, J Cereb Blood Flow Metab, 14 (1994) 783-801.

[70] H. Mure, S. Hirano, C.C. Tang, I.U. Isaias, A. Antonini, Y. Ma, V. Dhawan, D. Eidelberg, Parkinson's disease tremor-related metabolic network: characterization, progression, and treatment effects, NeuroImg, 54 (2011) 1244-1253.

[71] C. Huang, P. Mattis, K. Perrine, N. Brown, V. Dhawan, D. Eidelberg, Metabolic abnormalities associated with mild cognitive impairment in Parkinson disease, NEUROLOGY NEUROLOGY, 70 (2008) 1470-1477.

[72] J.H. Ko, H. Mure, C.C. Tang, Y. Ma, V. Dhawan, P. Spetsieris, D. Eidelberg, Parkinson's Disease: Increased Motor Network Activity in the Absence of Movement, Journal of Neuroscience, 33 (2013) 4540-4549.

[73] J.H. Ko, A. Feigin, P.J. Mattis, C.C. Tang, Y. Ma, V. Dhawan, M.J. During, M.G. Kaplitt, D. Eidelberg, Network modulation following sham surgery in Parkinson's disease, J Clin Invest, 124 (2014) 3656-3666.

[74] S. Peng, Y. Ma, P.G. Spetsieris, P. Mattis, A. Feigin, V. Dhawan, D. Eidelberg, Characterization of disease-related covariance topographies with SSMPCA toolbox: Effects of spatial normalization and PET scanners, Hum Brain Mapp, 35 (2014) 1801-1814.

[75] S. Craft, L.D. Baker, T.J. Montine, S. Minoshima, G.S. Watson, A. Claxton, M. Arbuckle, M. Callaghan, E. Tsai, S.R. Plymate, P.S. Green, J. Leverenz, D. Cross, B. Gerton, Intranasal Insulin Therapy for Alzheimer Disease and Amnestic Mild Cognitive Impairment A Pilot Clinical Trial, Archives of Neurology, 69 (2012) 29-38.

[76] M. Gold, P.A. Newhouse, D. Howard, R.J. Kryscio, NICOTINE TREATMENT OF MILD COGNITIVE IMPAIRMENT: A 6-MONTH DOUBLE-BLIND PILOT CLINICAL TRIAL, Neurology, 78 (2012) 1895-1895.

[77] I. Hajar, M. Hart, Y.-L. Chen, W. Mack, V. Novak, H.C. Chui, L. Lipsitz, Antihypertensive Therapy and Cerebral Hemodynamics in Executive Mild Cognitive Impairment: Results of a Pilot Randomized Clinical Trial, Journal of the American Geriatrics Society, 61 (2013) 194-201.

[78] C.M. Burns, K.W. Chen, A.W. Kaszniak, W. Lee, G.E. Alexander, D. Bandy, A.S. Fleisher, R.J. Caselli, E.M. Reiman, Higher serum glucose levels are associated with cerebral hypometabolism in Alzheimer regions, Neurology, 80 (2013) 1557-1564.

[79] J. Vina, A. Lloret, Why Women Have More Alzheimer's Disease Than Men: Gender and Mitochondrial Toxicity of Amyloid-beta Peptide, Journal of Alzheimers Disease, 20 (2010) S527-S533.

[80] K. Ishii, PET Approaches for Diagnosis of Dementia, American Journal of Neuroradiology, 35 (2014) 2030.

[81] A.K. Kono, K. Ishii, K. Sofue, N. Miyamoto, S. Sakamoto, E. Mori, Fully automatic differential diagnosis system for dementia with Lewy bodies and Alzheimer's disease using FDG-PET and 3D-SSP, European Journal of Nuclear Medicine and Molecular Imaging, 34 (2007) 1490-1497.

[82] Y. Chiba, E. Iseki, H. Fujishiro, K. Ota, K. Kasanuki, M. Suzuki, Y. Hirayasu, H. Arai, K. Sato, Early differential diagnosis between Alzheimer's disease and dementia with Lewy bodies: Comparison between F-18-FDG PET and I-123-IMP SPECT, Psychiatry Research-Neuroimaging, 249 (2016) 105-112.

[83] J.H. Ko, C.S. Lee, D. Eidelberg, Metabolic network expression in parkinsonism: Clinical and dopaminergic correlations, J Cereb Blood Flow Metab, 37 (2017) 683-693.

[84] K.A. Johnson, D.M. Rentz, E.K. Moran, J.A. Becker, M.G. Schlossmacher, R.S.Y. Lewis, A.J. Fischman, Combined dopamine transporter and FDG PET IN DLB, AD, and PD, Neurobiology of Aging, 25 (2004) S86-S87.

[85] J.R. Brosch, M.R. Farlow, S.L. Risacher, L.G. Apostolova, Tau Imaging in Alzheimer's Disease Diagnosis and Clinical Trials, Neurotherapeutics, 14 (2017) 62-68.

[86] E. Mohandas, V. Rajmohan, Frontotemporal dementia: An updated overview, Indian Journal of Psychiatry, 51 (2009) S65-S69.

[87] J.D. Warren, J.D. Rohrer, M.N. Rossor, Frontotemporal dementia, BMJ : British Medical Journal, 347 (2013).

[88] R.K.J. Brown, N.I. Bohnen, K.K. Wong, S. Minoshima, K.A. Frey, Brain PET in Suspected Dementia: Patterns of Altered FDG Metabolism, RadioGraphics, 34 (2014) 684-701.

[89] L.T. Grinberg, H. Heinsen, Toward a pathological definition of vascular dementia, Journal of the Neurological Sciences, 299 (2010) 136-138.

[90] C.M.D. Patterson, J.W.M.D.M. Feightner, A.M.D.P. Garcia, G.Y.R.M.D.M. Hsiung, C.M.D.M. MacKnight, A.D.P. Sadovnick, Diagnosis and treatment of dementia: 1. Risk assessment and primary prevention of Alzheimer disease, Canadian Medical Association. Journal, 178 (2008) 548-556.